Indonesian Journal of Physics
Vol 22 No. 3, July 2011

The Change in Physical Properties of $Bi_2Ca_2Co_2O_8$ Thermoelectric Materials Induced by Pb and Rare-Earth Dopings

Inge Magdalena Sutjahja
Physics of Magnetism and Photonic Research Divison,
Faculty of Mathematics and Natural Sciences,
Institut Teknologi Bandung,
e-mail : inge@fi.itb.ac.id

Received 13 Febaruary 2011, Revised 19 April 2011, Accepted 26 May 2011

Abstract

We report in this paper the change in the physical properties due to dopant effect in $Bi_2Sr_2Co_2O_8$ parent compound system. The doped samples consists of Pb-doped samples ($Bi_{2-x}Pb_xSr_2Co_2O_8$, x = 0, 0.5, 1.0, 1.5, and 2.0) and RE-doped samples ($Bi_{2-x}Pb_xCa_{1.9}RE_{0.1}Co_2O_8$, RE = Y, La, Pr, Sm, Eu, Gd, and Ho). The structure of this layered oxide system consist of an alternate stack of CoO_2 layer and $Bi_2Sr_2O_4$ block along the c*-axis with misfit structure along* b*-direction. From the analysis of XRD data it is found that the* c*-axis parameter reduced significantly in the RE-doped samples compared with those of Pb-doped samples, while the value of misfit degree almost the same. The changes in these lattice structures are accompanied by variation in the spin-state of Co-ions and electrical conductivity. We argue that these structural changes and its effect on the electrical transport properties as well as control of the magnetism plays a pivotal role in determining the thermopower in this class of magnetic thermoelectric materials through the entropy of the charge carriers. This, in turn, will determine the thermoelectric performance for application.*

Keywords: *Thermoelectric material; Misfit structure; Spin-state of Co-ions; Electrical conductivity; Thermopower (Seebeck coefficient).*

1. Introduction

Among the currently developed alternative energy sources, the thermoelectric (TE) material based system offers the unique ability of direct conversion of thermal energy to electrical energy and vise versa, without producing undesirable environmental effects. The thermoelectric material is a material that can generate electricity from heat through the Seebeck effect. The performance of thermoelectric devices is characterized by its figure of merit (FOM), which is defined by $ZT = (S^2\sigma/\kappa)T$, where T is the operating temperature, S the thermopower or Seebeck coefficient, σ (= $1/\rho$) is the electrical conductivity (inverse resistivity) and κ is the thermal conductivity. Thus, to reach the technology application scale (ZT > 1), one have to manipulate the charge carrier concentration through doping to have the large values of S and σ, while reducing the κ value. In general, this demand is rarely found in normal metal or semiconductor materials because the three parameters cannot be controlled independently[1].

However, since the discovery of good thermoelectric properties in layered cobalt oxide Na_xCoO_2 [2], oxides thermoelectric have been intensively investigated and several new systems have been found, such as $Sr_3YCo_4O_y$ [3], $La_{1-x}Sr_xCoO_3$ [4], $Ca_3Co_4O_9$ [5], and $Bi_2Sr_2Co_2O_y$ [6]. Figure 1 shows the crystal structures of various layered cobalt oxides, all of them consists of the CdI_2-type CoO_2 block that is a key ingredient for good thermoelectricity, which alternately stacks with various block layers along the *c*-axis[7]. This structure is essentially the same with those of high-temperature superconducting copper oxides, except for the lattice misfit between the CoO_2 and block layer[8].

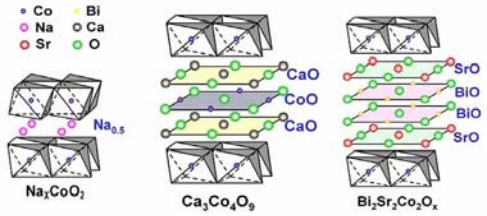

Figure 1. The crystal structure of the various layered cobalt oxides.

In this article we show the change in physical properties of $Bi_2Sr_2Co_2O_8$ parent compound due to dopant effect. The investigations based on the correlation study of crystal structure, magnetic, and electrical transport data. The samples consists of Pb-doped samples ($Bi_{2-x}Pb_xSr_2Co_2O_8$ with x = 0, 0.5, 1.0, 1.5, and 2.0) and RE-doped samples ($Bi_{2-x}Pb_xCa_{1.9}RE_{0.1}Co_2O_8$ with RE = Y, La, Pr, Sm, Eu, Gd, and Ho).

2. Theoretical Background

Intensive studies show that the physical mechanism behind the good thermoelectricity in cobalt-oxide systems is different with those of conventional semiconductor. According to the Boltzmann transport equation, the electrical current

density $\vec{j}$ and the thermal current density $\vec{q}$ are expressed by linear combinations of the electric field $\vec{E}$ and the temperature gradient $-\vec{\nabla}T$ as [9]:

$$\vec{j} = \sigma\vec{E} + \sigma S\left(-\vec{\nabla}T\right)$$
$$\vec{q} = \sigma ST\vec{E} + \kappa'\left(-\vec{\nabla}T\right) \quad (1)$$

where κ' is the thermal conductivity without electric field. In the absence of the temperature gradient, equation (1) will reduce to

$$\frac{\vec{q}}{T} = S\vec{j} \quad (2)$$

Thus, from the last equation one may conclude that the thermopower S is the ratio of the entropy current to the electrical current. If the two relaxation times contained in $\vec{j}$ and $\vec{q}$ are assumed to be the same, the thermopower can be regarded as an entropy per charge, or the so called "transport entropy". Taking into account the orbital and spin degrees of freedom together with strong electron correlations, Koshibae have derived the expression of the thermopower as[10]

$$S = -\frac{k_B}{e}\ln\left(\frac{g_3}{g_4}\frac{x}{1-x}\right) \quad (3)$$

where g_3 (g_4) are the degeneracies of the Co^{3+} (Co^{4+}) ions in the splitted t_{2g} and e_g orbitals originated from 5-degenerate 3*d*-orbital under the influence of crystal field effect, and x is the doping content. According to the spin total value (S), three different spin-states are denoted as low-spin (LS), intermediate-spin (IS), and high-spin (HS) states, as clearly shown in Fig. 2.

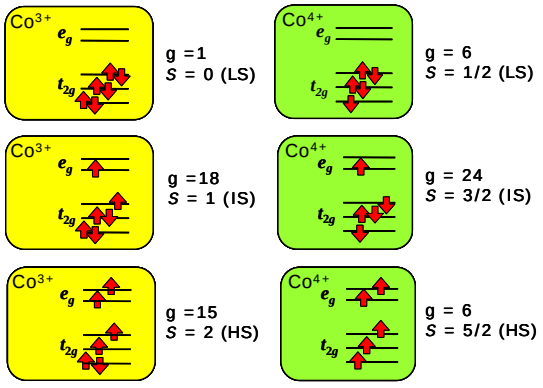

Figure 2. The local electronic state of the Co^{3+} (3*d*) and Co^{4+} (3*d*) ions in the splitted t_{2g} and e_g orbital, and g is the total degeneracy number.

The spin-state of the Co-ions can be tuned, for example, from the magnetic measurements. This phenomenological model can successfully predict the sign and values of thermopower in several transition-metal based systems. Particularly, in Na_xCoO_2 system it was found that the spin-state of Co-ions (Co^{3+} and Co^{4+}) are in the low-spin (LS) state, since the crystal field splitting is large enough to overcome the Hund's coupling. Thus, from the electronic configurations of Co^{3+} and Co^{4+} ions in the splitted t_{2g} and e_g orbitals, the transport entropy value is estimated to be $k_B \ln 6/|e| = 150\mu V/K$, which is roughly equal to the experimental thermopower value at high temperatures[10].

3. Experimental

Magnetic thermoelectric materials of doped-$Bi_2Sr_2Co_2O_8$ parent compound consists of Pb-doped $Bi_{2-x}Pb_xSr_2Co_2O_8$ (x = 0, 0.5, 1.0, 1.5, 2.0) or the so-called (Bi,Pb)-2228 and RE-doped samples ($Bi_{1.5}Pb_{0.5}Ca_{1.9}RE_{0.1}Co_2O_8$, RE = Y, La, Pr, Sm, Eu, Gd, and Ho). The samples have been prepared separately from precursors of Bi_2O_3, PbO, $CaCO_3$, Y_2O_3, RE_2O_3 and Co_3O_4 by conventional solid state reaction method. The precursors were pulverized by ball milling for several hours, followed by calcination and sintering in air at various temperatures for about several hours. Complete description about synthesis procedure as well as its phase and structure characterization have been published elsewhere[11,12].

The structural analyses are performed based on the XRD measurements data. The magnetic susceptibility measurements were done by using PPMS in the ZFC mode with applied field of 1000 Oe and in the temperature range between 5 and 300 K. The measurements of electrical resistivity were carried out using the experimental set-up of closed-cycle refrigerator and automatic LABVIEW program that has been available in our laboratory.

4. Experimental Data and Analysis

4.1 Structural measurement analysis

The XRD data of the Pb-doped $Bi_{2-x}Pb_xSr_2Co_2O_8$ (x = 0, 0.5, 1.0, 1.5, 2.0) and RE-doped ($Bi_{1.5}Pb_{0.5}Ca_{1.9}RE_{0.1}Co_2O_8$, RE = Y, La, Pr, Sm, Eu, Gd, and Ho) samples as well as its refinement results using Rietica 2007 program have been published separately [11,12]. Hence, for short, we show only in Table 1 and Table 2 the results for lattice parameters along with doping variations. The cell parameters are represented by (a_1, b_1, c_1, β_1) and (a_2, b_2, c_2, β_2), each of them belongs to the block layer and the CoO_2 sublattices, in accordance with the structure shown in Figure 1. We found that, within the accuracy of the refinement, $a_1 = a_2 = a$, $c_1 = c_2 = c$, and $\beta_1 = \beta_2 = \beta$, while $b_1 \neq b_2$, which reveals the misfit character of the structure. The ratio value of b_2/b_1 marks the misfit degree of the structure.

Table 1. The variations of lattice constants with the amount of Pb-doping.

x	a (Å)	b_1 (Å)	c (Å)	b_2 (Å)	β (deg)	b_2/b_1
0	5.06	5.2397	29.8916	2.8259	93.4956	0.53932
0.5	4.99	5.1807	29.8507	2.7881	93.0074	0.53817
1.0	4.986	5.1528	29.8423	2.8126	92.6834	0.54584
1.5	4.978	5.1992	29.8229	2.8098	92.3511	0.54043
2.0	4.8689	5.2110	29.7657	2.7703	92.2515	0.53163

Table 2. The variations of lattice constants with the type of RE-doping.

RE	a (Å)	b_1 (Å)	c (Å)	b_2 (Å)	β (deg)	b_2/b_1
Y	5.1217	5.2161	29.4522	2.7975	92.8246	0.537
La	5.0746	5.2109	29.3865	2.8711	92.8330	0.55098
Pr	5.0763	5.2235	29.3984	2.8833	92.9865	0.55199
Sm	5.0843	5.2235	29.3994	2.8833	92.9868	0.55199
Eu	5.0854	5.2240	29.4308	2.8882	92.9881	0.55287
Gd	5.0897	5.2253	29.4320	2.8896	92.989	0.553
Ho	5.0913	5.2297	29.4472	2.8901	92.9967	0.55263

From these tables one can see the reduction of the *c*-axis lattice parameter in the case of RE-doped samples compared with those of Pb-doped samples. We note that this reduction might be due to smaller ionic radii of Ca^{2+} ions compared with Sr^{2+} ions or the effect of rare-earth doping. Besides that, the degree of lattice misfit almost the same in those two kinds of samples.

4.2 Magnetization measurement data and analysis

The inverse molar susceptibility versus temperature curves of the Pb-doped and RE-doped samples are presented in Figure 3. We note that there is no anomaly or transition for the Pb-doped samples as shown by the data in Figure 3(a). However, it is seen that the high temperature part ($T > 200$ K) of the data that show straight lines that obeys the Curie-Weiss law[13]. On the other hand, the RE-doped samples with RE = Sm show a clear magnetic transition at temperature around 50 K, although it is not a sharp transition and it can't be observed in the specific-heat and electrical resistivity measurements in the limit of apparatus resolution. We note that the origin of this anomaly is not known yet, and it needs other measurements for clarification. In other side, the low-temperature broad anomaly observed in La-doped samples is similar with the anomaly observed in other La-compound such as $La_{0.85}Sr_{0.15}CoO_3$ [14], which might be due to spin-glass ordering of La^{3+}-ions. In this case, a large hysteresis might be observed between the data taken in the ZFC and FC modes.

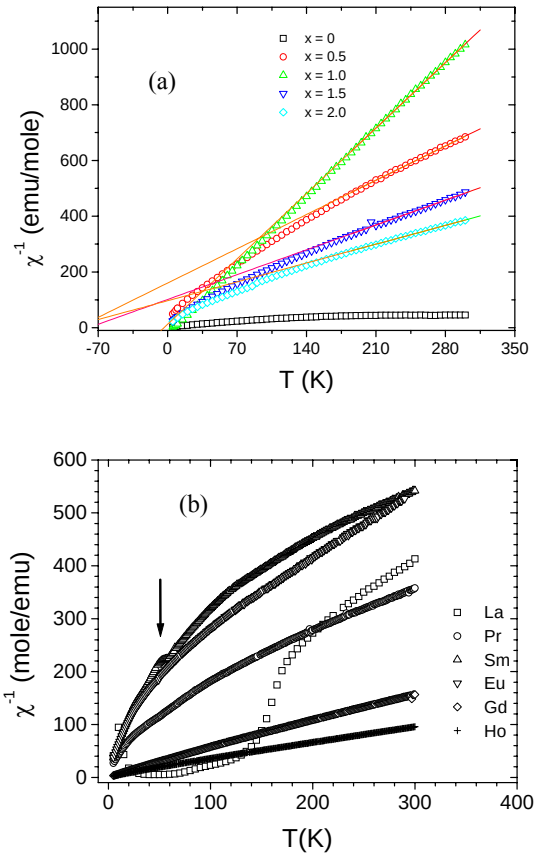

Figure 3. The The inverse molar susceptibility versus temperature ($\chi^{-1} - T$) of: (a) Pb-doped and (b) RE-doped samples. In Fig (a) the solid lines are the linear fit of the data at high temperatures above 200 K. The arrow in Fig (b) point the anomaly for RE = Sm at temperature around 50 K.

In follows, the effective magnetic moment per Co ion, μ_{eff}, can be obtained from the slope of the straight line or the so called Curie constant. The resulted plot of μ_{eff} for two kinds of samples are shown in Figure 4. These experimental μ_{eff} values are then compared with the theoretical values, following the formula $\mu_{eff} = g\left[J(J+1)\right]^{1/2}\mu_B$, where g = 2 is the Lande's g factor and J is the total quantum number, which is equal to the total spin quantum number ($J = S_{\text{spin}}$) of the Co-ions due to orbital quenching [15]. In the next step, we fit the experimental data with the theoretical curves, assuming the different spin-state configuration of Co-ions, namely Co^{3+} and Co^{4+} ions, each of them with different number of spin total (S_3 and S_4), in such a way that $S_{\text{spin}} = (2\text{-}x)\,S_3 + x\,S_4$, with x is doping concentration[15].

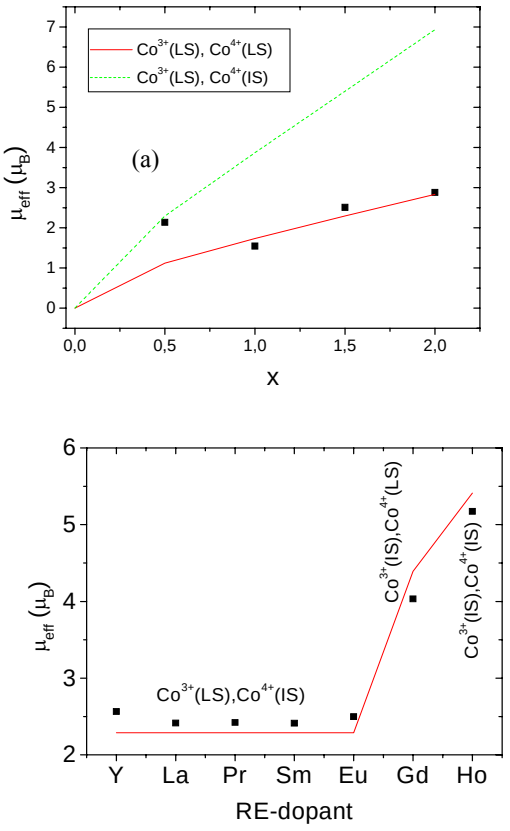

Figure 4. The effective magnetic moment μ_{eff} values of: (a) Pb-doped and (b) RE-doped samples obtained from the experimental data. The solid lines represent the theoretical μ_{eff} by assuming the different spin-state of Co^{3+} and Co^{4+} ions (see text for further explanation).

As shown as solid and dashed lines in Figure 4, for each investigated sample the experimental effective magnetic moment μ_{eff} of Co-ions is best fitted theoretically by assuming different spin-state variation of Co-ions. In Pb-doped samples, both of the Co^{3+} and Co^{4+} ions are in the low-spin (LS) state [16]. The RE-doped samples show rich variation of spin-state of Co-ions: for lighter dopant elements of Y, La, Pr, Sm and Eu, each of the Co^{3+} and Co^{4+} ions are in the low-spin (LS) and intermediate-spin (IS) state, respectively. More interestingly, spin-state variation is found in heavier dopant elements of Gd and Ho, namely : Co^{3+} (IS) and Co^{4+} (LS) for RE = Gd and Co^{3+} (IS) and Co^{4+} (IS) for RE = Ho. We argue that, these variations of spin-state of Co-ions might be due to the effect of other d- and/or f-electrons originated from dopant.

4.3 Electrical resistivity data

In general the electrical resistivity data of the Pb-doped and RE-doped samples, as shown in Figure 3, show insulating behavior. We found that in Pb-doped samples, Pb doping reduced the resistivity values rather significantly (inset of Figure 5(a)), due to increase of charge carrier concentration (holes) by Pb^{2+} doping to Bi^{3+}. We note that the value of resistivity in RE-doped samples without RE doping, namely $Bi_{1.5}Pb_{0.5}Ca_2Co_2O_8$, is about one order of magnitude smaller than the resistivity value of undoped $Bi_2Sr_2Co_2O_8$. In opposite with the effect of Pb doping, the values of resistivity are enhanced by RE-doping, giving a clue for the reduction of charge carrier concentration in this RE-doping samples. We note that for RE = La, the magnitude of electrical resistivity is almost the same with its parent compound $Bi_2Sr_2Co_2O_8$, namely in the order of 100 Ωcm. Qualitatively, this phenomena might be due to charge carrier competition, namely between the holes (from Pb^{2+} doping to Bi^{3+}) and electrons (due to RE^{3+} doping to Ca^{2+}). We further note that the insulator to metal transition is clearly observed at high temperature about 200 K for RE = La, similar with the spin-glass system of $La_{0.85}Sr_{0.15}CoO_3$ [14]. The origin for this transition and its effect with the applied magnetic field will be described elsewhere.

It is interesting at this point, to relate the above structural, magnetic, and transport data. From the magnetic measurement, the spin state of the Co-ions in Pb-doped samples are in the low-spin state, or the crystal field splitting is large enough to overcome Hund's coupling. Thus, the electronic configuration of Co^{3+} and Co^{4+} ions are $(t_{2g})^6$ and $(t_{2g})^5$. For the Co^{3+} ions, with six electrons fully occupy the triply degenerate t_{2g} orbital, the charge entropy is zero. In other words, in this particular samples the charge carriers are due to unfilled electrons belongs to Co^{4+} ions. In other side, the reduction of electrical resistivity in RE-doped samples are in conjunction with the reduction of the c-axis lattice parameter, namely a higher probability for the charge carrier to tunnel along the layers. This might be also connected to rich variation of the spin-state of the Co-ions. For example, for RE = Y, La, Pr, Sm, Eu, where the spin state of Co^{3+} and Co^{4+}-ions are LS and IS, respectively, thus the conductivity is due to electrons belongs to Co^{4+} ions in the unfilled e_g and t_{2g} orbital.

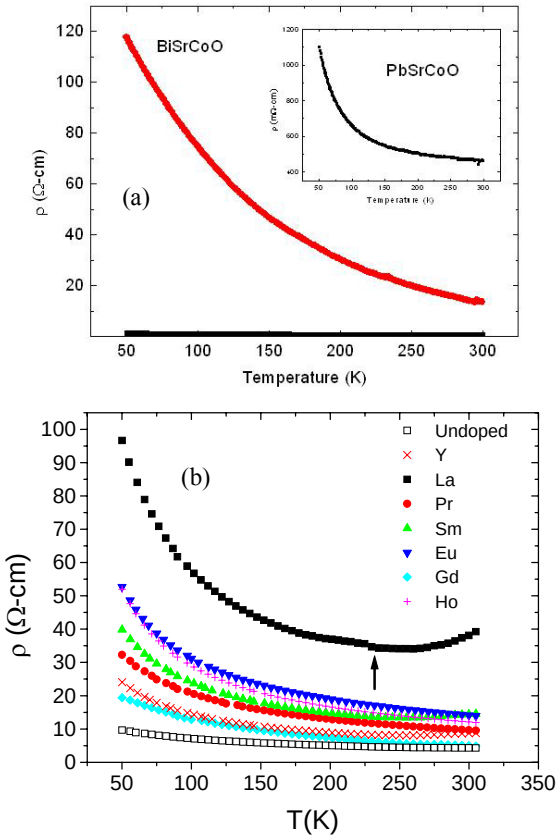

Figure 5. The electrical resistivity data of the (a) Pb-doped and (b) RE-doped samples. The inset of Figure (a) show the resistivity of the $Pb_2Sr_2Co_2O_8$. The arrow in Figure (b) show the insulator to metal transition for RE = La.

We argue further, that the different doping effects of these two kinds of samples on the crystal structure, magnetic, and electrical transport should also affect the thermopower (Seebeck coefficient) and thermal conductivity. These data are needed to determine its performance for application.

5. Summary

We have presented in this paper the doping effect on the physical properties of the doped-$Bi_2Sr_2Co_2O_8$ parent compound samples through the correlation study of the crystal structure, magnetic, and electrical transport data. The investigations are devoted to Pb^{2+} doping effect on the Bi^{3+} ($Bi_{2-x}Pb_xSr_2Co_2O_8$, x = 0, 0.5, 1.0, 1.5, 2.0) and RE^{3+} doping on the Ca^{2+} ($Bi_{1.5}Pb_{0.5}Ca_{1.9}RE_{0.1}Co_2O_8$, RE = Y, La, Pr, Sm, Eu, Gd, and Ho). In the RE-doped samples, the *c*-axis lattice parameters reduced significantly while the misfit degree almost the same compared with those of Pb-doped samples. In this RE-series of samples, various spin state of the Co^{3+} and Co^{4+} ions are deduced from the magnetization data. Moreover, the values of electrical resistivity are in between those of undoped $Bi_2Sr_2Co_2O_8$ parent compound and fully Pb-doped $Pb_2Sr_2Co_2O_8$ due to charge carrier competition. We argue that in the RE-doping samples the transport entropy is affected by the *d*- and/or *f*-electrons belongs to rare-earth ions, which is enhanced by the change in the crystal structure and tunneling mechanism along the *c*-axis direction. Further thermopower (Seebeck coefficient) and thermal conductivity data are in progress for the eventual evaluation of the material's FOM.

Acknowledgements

The XRD and magnetic susceptibility measurements were performed in Japan (University of Osaka). Part of this work was supported by Riset Ikatan Alumni ITB 2010 under contract No. 1443c/K01.7/PL/2010 and Riset dan Inovasi KK ITB 2011 under contract No. 223/I.1.C01/PL/2011.

References

1. G. Mahan, B. Sales, and J. Sharp, Thermoelectric Materials: New Approaches to an Old Problem, *Physics Today March,* **50,** 42, 1997.
2. I. Terasaki, Y. Sasago, and K. Uchinokura, Large thermoelectric power in $NaCo_2O_4$ single crystals, *Phys. Rev. B*., **56,** 12, 685, 1997.
3. W. Kobayashi, *et al*., Room-temperature ferromagnetism in $Sr_{1-x}Y_xCoO_{3-\delta}$ ($0.2 \le x \le 0.25$), *Phys. Rev. B*., **72**, 104408, 2005.
4. K. Berggold, *et al*., Thermal conductivity, thermopower, and figure of merit of $La_{1-x}Sr_xCoO_3$, *Phys. Rev. B*., **72**, 155116, 2005.
5. A. Maignan, *et al*., Magnetoresistance and magnetothermopower properties of Bi/Ca/Co/O and Bi(Pb)/Ca/Co/O misfit layer cobaltites, *J. Phys.*: *Condens. Matter*, **15**, 2711, 2003.
6. R. Funahashi, I. Matsubara, and S. Sodeoka, Thermoelectric properties of $Bi_2Sr_2Co_2O_x$ polycrystalline materials, *Appl. Phys. Lett.* **76**, 2385, 2000; R. Funahashi and M. Shikano, $Bi_2Sr_2Co_2O_y$ whiskers with high thermoelectric figure of merit, *Appl. Phys. Lett.* **81**, 1459, 2002.
7. Qiang Li, On the Thermoelectric Properties of Layered Cobaltates, *Mater. Res. Soc. Symp. Proc.* Vol. 886 © 2006 Materials Research Society.
8. H. Leligny, *et al*., *A five-dimensional structural investigation of the misfit layer compound* $[Bi_{0.87}SrO_2]_2[CoO_2]_{1.82}$, Acta Crystallographica Section B, **56**, 173-182, 1999.
9. I. Terasaki, *et al*., Novel thermoelectric properties of complex transition-metal oxides, *Dalton Transactions*, **39**(4), 1005-1011, 2010.
10. W. Koshibae, T. Tsutsui and S. Maekawa, Thermopower in cobalt oxides, *Phys. Rev. B*., **62**, 6869, 2000.
11. I.M. Sutjahja, *et al*., Synthesis and Characterization Magnetic Thermoelectric Materials of $Bi_{2-x}Pb_xSr_2Co_2O_8$, Proceeding of the ICMNS Conference, FMIPA-ITB, October 2008.

12. I.M. Sutjahja, T. Akbar, A.A. Nugroho, Lanthanide Contraction Effect in Magnetic Thermoelectric Materials of Rare Earth-doped $Bi_{1.5}Pb_{0.5}Ca_2Co_2O_8$, Proceeding of the Asian Physics Symposium (APS 2010), July 22 – 23, 2009, Bandung, Indonesia, published in AIP (American Institute of Physics), 2011.
13. C. Kittel, Introduction to Solid State Physics, seventh ed., John Wiley & Sons, Inc., 1996.
14. P A Joy and S K Date, Metal-insulator transition in the spin-glass system $La_{0.85}Sr_{0.15}CoO_3$, *J. Phys.: Condens. Matter*., **11(**21), L217-L221, 1999.
15. X. Xu, *et al*., Relationship between spin state of Co ions and thermopower in $La_{1-x}Sr_xCoO_3(0\leq x\leq 0.5)$, *Phys. Lett. A*., **351**, 431-434, 2006.